Brain Struct Funct (2012) 217:49–61
DOI 10.1007/s00429-011-0323-z

ORIGINAL ARTICLE

# Neurodegeneration in the somatosensory cortex after experimental diffuse brain injury

**Jonathan Lifshitz · Amanda M. Lisembee**

Received: 21 December 2010 / Accepted: 28 April 2011 / Published online: 20 May 2011


**Abstract** Disruption and consequent reorganization of central nervous system circuits following traumatic brain injury may manifest as functional deficits and behavioral morbidities. We previously reported axotomy and neuronal atrophy in the ventral basal (VB) complex of the thalamus, without gross degeneration after experimental diffuse brain injury in adult rats. Pathology in VB coincided with the development of late-onset aberrant behavioral responses to whisker stimulation, which lead to the current hypothesis that neurodegeneration after experimental diffuse brain injury includes the primary somatosensory barrel cortex (S1BF), which receives projection of VB neurons and mediates whisker somatosensation. Over 28 days after midline fluid percussion brain injury, argyrophilic reaction product within superficial layers and layer IV barrels at 1 day progresses into the cortex to subcortical white matter by 7 days, and selective inter-barrel septa and subcortical white matter labeling at 28 days. Cellular consequences were determined by stereological estimates of neuronal nuclear volumes and number. In all cortical layers, neuronal nuclear volumes significantly atrophied by 42–49% at 7 days compared to sham, which marginally attenuated by 28 days. Concomitantly, the number of healthy neurons was reduced by 34–45% at 7 days compared to sham, returning to control levels by 28 days. Progressive neurodegeneration, including argyrophilic reaction product and neuronal nuclear atrophy, indicates injury-induced damage and reorganization of the reciprocal thalamocortical projections that mediate whisker somatosensation. The rodent whisker barrel circuit may serve as a discrete model to evaluate the causes and consequences of circuit reorganization after diffuse brain injury.

**Keywords** Disector · Fractionator · Nucleator

## Introduction

Discrete neural circuits sub-serve specific neurological functions. In the wake of traumatic brain injury (TBI), neural circuits may be destroyed or damaged by the primary mechanical forces or ensuing degenerative events. Circuit destruction leads to obvious functional deficits or impairment (Glassman 1994). On the other hand, circuit disruption and consequent reorganization can evolve into behavioral morbidity with the formation of maladaptive circuits (Steward 1989), as evidenced by the delayed onset of post-traumatic seizure (Pitkanen et al. 2009). Circuit disruption in the thalamus, due to diffuse axotomy, likely perturbs ascending thalamocortical sensory and descending corticothalamic pathways, in addition to intracortical executive functions (Uzan et al. 2003; Maxwell et al. 2004; Reeves et al. 2005). In this way, enduring post-traumatic morbidities span the neurological spectrum from cognition

**Electronic supplementary material** The online version of this article (doi:10.1007/s00429-011-0323-z) contains supplementary material, which is available to authorized users.

J. Lifshitz (✉) · A. M. Lisembee
Spinal Cord and Brain Injury Research Center (SCoBIRC), University of Kentucky Chandler Medical Center, Office B463, Biomedical and Biological Sciences Research Building, 741 S. Limestone St, Lexington, KY 40536-0509, USA
e-mail: JLifshitz@uky.edu

J. Lifshitz
Department of Anatomy and Neurobiology, University of Kentucky College of Medicine, Lexington, KY, USA

J. Lifshitz
Department of Physical Medicine and Rehabilitation, University of Kentucky College of Medicine, Lexington, KY, USA

to emotion, resulting in staggering personal and societal costs (Langlois et al. 2004). Investigating the natural course of circuit damage, degeneration and reorganization are essential to guide potential therapeutic interventions or clinical treatment after TBI.

Diffuse axonal injury begins with focal impairment of axonal transport, resulting in progressive swelling and then delayed disconnection (Biasca and Maxwell 2007), often found within 60–100 μm of the soma (Singleton and Povlishock 2004; Kelley et al. 2006). In diffuse brain injury uncomplicated by contusion, atrophy of individual neurons, rather than their loss, is the predominant neuropathological consequence of axotomy (Singleton et al. 2002; Lifshitz et al. 2007; Greer et al. 2011). More than 3 months after human TBI, similar neuronal atrophy, in addition to loss, has been documented across cortical domains, despite heterogeneous injury mechanisms, clinical complications, and varying mean post-injury survival time points (Maxwell et al. 2010). Hence, in addition to axotomy, somal perturbation across brain regions may be a histopathological hallmark of experimental and clinical TBI. The possibility remains for early and transient neuronal perturbation to trend toward recovery (Povlishock 1986; Singleton et al. 2002; Lifshitz et al. 2007), with the caveat that unguided reorganization could develop maladaptive circuits that underlie post-traumatic morbidities. Axotomy and reorganization likely explain the regional atrophy (Warner et al. 2010) and widespread activation patterns during functional imaging (Christodoulou et al. 2001; Levine et al. 2002) observed following diffuse TBI in humans.

For the rodent, whisker somatosensation is a primary sense, aiding in spatial navigation by tactile surface detection. Sensory information from the mystacial whiskers projects to the ipsilateral principle trigeminal nucleus, then crosses the midline to the contralateral ventral posterior medial (VPM) nucleus of the thalamus, and on to barrel fields in layer IV of primary sensory cortex (S1BF) (Woolsey and Van der 1970; O'Leary et al. 1994). Each cortical barrel is an element of a functional sensory input column that spreads from layer II/III to layer VI (Waite and Tracey 1995; Giaume et al. 2009). This whisker barrel circuit provides anatomical landmarks and discrete sensory function to evaluate the neuropathological consequences of diffuse TBI. The primary mechanical injury forces result in diffuse axonal injury and perisomatic axotomy (Kelley et al. 2006; Lifshitz et al. 2007), particularly within the VPM, that would disconnect thalamocortical projection neurons. Acutely, whisker stimulation results in attenuated neuronal activation, which later recruits broader and greater thalamic and cortical activation (Hall and Lifshitz 2010). It follows that whisker stimulation in the awake brain-injured rodent elicits aberrant behavioral responses at and beyond 1-month post-injury (McNamara et al. 2010), suggestive of the agitated behaviors often observed in survivors of brain injury (Waddell and Gronwall 1984; Bohnen et al. 1991).

Accordingly, the current study explores the time course and subregional localization of neurodegeneration in the S1BF after diffuse brain injury as predicted by the pathology in the VPM thalamic relay (Lifshitz et al. 2007), functional hyperactivation in VPM and S1BF to whisker stimulation (Hall and Lifshitz 2010) and development of aberrant behaviors upon whisker stimulation (McNamara et al. 2010). In brain-injured and uninjured rats over 1 month after moderate midline fluid percussion brain injury, we demonstrate injury-induced neurodegeneration progressing through the cortical layers into subcortical white matter as indicated by accumulation of argyrophilic reaction product, reduction in healthy neuronal number and atrophy of neuronal nuclear volumes. These results provide quantitative insights to cortical layer specific consequences of circuit disruption that may contribute to the development of behavioral morbidity.

## Materials and methods

### Midline fluid percussion brain injury

Adult male Sprague–Dawley rats (375–400 g) were subjected to midline fluid percussion injury (FPI) consistent with methods described previously (Lifshitz 2008; Hosseini and Lifshitz 2009). Briefly, rats were anesthetized with 4% isoflurane in 70% $N_2O$ and 30% $O_2$, intubated, and maintained on a ventilator with 2% isoflurane. For some animals, anesthesia was delivered in 100% $O_2$, without intubation. During surgery, body temperature was maintained at 37°C with a thermostat-controlled heating pad (Harvard Apparatus, Holliston, MA). In a head holder assembly (Kopf Instrument, Tujunga, CA), a midline scalp incision exposed the skull. A 4.8-mm circular craniotomy was performed (centered on the sagittal suture midway between bregma and lambda) without disrupting the underlying dura or superior sagittal sinus. An injury cap was fabricated from the female portion of a Leur-Loc needle hub, which was cut, beveled, and scored to fit within the craniotomy. Skull screws were secured in 1-mm holes hand-drilled into the right frontal (+2.0 mm rostral, +2.0 mm lateral from bregma) and occipital (−2.0 mm posterior, 0.0 mm lateral from lambda) bones. The injury hub was affixed over the craniotomy using cyanoacrylate after which methyl-methacrylate (Hygenic Corp., Akron, OH) was applied around the injury hub and screws. The scalp was sutured closed over the hub and cured adhesive, topical Lidocaine ointment was applied, and the animal

was extubated. Animals were returned to a warmed holding cage and monitored until ambulation returned.

For the injury induction, animals were re-anesthetized with 4% isoflurane approximately 60–90 min after the conclusion of the surgical procedure. The incision was opened and the female end of the injury hub assembly was filled with normal saline and was attached to the male end of the fluid percussion device (Custom Design and Fabrication, Virginia Commonwealth University, Richmond, VA). An injury of moderate severity (1.91 ± 0.02 atm) was administered by releasing the pendulum onto the fluid-filled piston, moments before reflexive responses returned. After injury, the injury hub assembly was removed *en bloc*, bleeding was controlled with Gelfoam (Pharmacia, Kalamazoo, MI), and the incision was sutured. Animals were monitored for spontaneous respiration and the return of the righting reflex. After recovery of the righting reflex, animals were placed in a warmed holding cage before being returned to the vivarium. For sham-injured animals, the identical surgical procedures were followed, without the induction of the injury. All brain-injured animals had righting reflex recovery times >6 min (404 ± 22 s) compared to <15 s for sham-injured animals. Two additional animals died from respiratory complications caused by the injury over the course of the study. Experiments were conducted in accordance with National Institutes of Health (NIH) and Institutional Animal Care and Use Committee (IACUC) guidelines concerning the care and use of laboratory animals.

## Aminocupric silver technique

Argyrophilic reaction product, which has come to indicate neurodegeneration, was examined using the de Olmos aminocupric silver histochemical technique as previously described (de Olmos et al. 1994; Switzer 2000; Mikics et al. 2008). At designated times, sham ($n = 3$; one per time point) or brain-injured rats ($n = 3$ per time point) were overdosed with sodium pentobarbital (200 mg/kg i.p.) and transcardially perfused with 0.9% sodium chloride, followed by a fixative solution containing 4% paraformaldehyde and 4% sucrose in 0.1 M phosphate buffered saline. Following decapitation, the heads were stored in a fixative solution containing 15% sucrose for 24 h, after which the brains were removed, placed in fresh fixative, and shipped for histological processing to Neuroscience Associates Inc. (Knoxville, TN). The rat brains were embedded into a single gelatin block (Multiblock® Technology; Neuroscience Associates). Individual cryosections containing all the rat brains were mounted and stained with the de Olmos aminocupric silver technique according to proprietary protocols (Neuroscience Associates) to reveal argyrophilic reaction product, which localized to neurons and neuronal processes, counterstained with Neutral Red, and then cover-slipped. The stained sections were analyzed in our laboratory.

Quantification of the argyrophilic reaction product in the primary somatosensory barrel fields was conducted by calculating the percentage of argyrophilic-positive pixels from grayscale digital photomicrographs, comparable to the pixel quantification as previously described (Hall and Lifshitz 2010). Briefly, the primary somatosensory barrel cortex was divided into thirds through the depth of the cortical mantel (superficial, middle, deep) by tracing a 4× digital photomicrograph at approximately −2.3 mm from bregma. The absence of cytoarchitecture in the stain precluded analysis by traditional cortical layers. The grayscale pixel distribution was digitally thresholded to separate positive stained pixels from unstained pixels (BioQuant, BioQuant Image Analysis Corporation). The thresholded image was then segmented into white and black pixels, indicating positive and negative staining, respectively. Measurements were made in triplicate and averaged to calculate the silver staining (argyrophilic reaction product) as percent of positive silver stained pixels (white pixels) in the region of interest (white + black pixels).

## Stereology tissue preparation and Giemsa stain

Rats were euthanatized at 1 day ($n = 4$), 7 days ($n = 5$) or 28 days ($n = 5$) after brain or sham ($n = 4$; one per time point and two at 7 days) injury with an overdose of sodium pentobarbital (200 mg/kg, i.p.) and transcardially perfused with 0.9% NaCl followed by 4% paraformaldehyde/0.1% glutaraldehyde in sodium cacodylate buffer. The brains were removed and blocked in the coronal plane (12 mm extent in the rostral-caudal plane) and paraffin processed. Post-processing, brains were embedded, comprehensively sectioned at 30 μm in the coronal plane (Shandon, AS325, Waltham, MA), and wet mounted on 2% gelatin-subbed slides. Every other section was heated, deparaffinized, rehydrated, stained with 10% Giemsa stain (EM Sciences, #26156-01) at 60°C, differentiated with 1% acetic acid, dehydrated, and coverslipped. The histological sections are the same as those used to quantify the ventral basal complex in a previous study (Lifshitz et al. 2007).

## Design-based stereology

Design-based stereological estimates of neuronal nuclear volume, neuronal number, and regional volume were obtained by systematic-random sampling in layers II/III (relay), IV (input), and V (output) of the S1BF in one hemisphere of brain-injured and uninjured rats. For stereological analyses, the somatosensory barrel cortex

included layers II/III, IV, and V of the cortex from Bregma level −0.36 mm through −4.36 mm, according to the Paxinos and Watson rat brain atlas (Paxinos and Watson 1998). Briefly, measuring the diameter of a neuronal nucleus on a length cubed ruler at a random orientation allows for a mathematical estimate of nuclear volume (Gundersen 1988). Counting 150–200 neurons in a defined area of each tissue section, through a known depth of the tissue section, in a known fraction of tissue sections allows for a mathematical estimate of the total population of neurons, as described below. Counting the number of systematically random points falling within a region of interest provides an estimate of area, which can be extrapolated to regional volume based on the Cavalieri principle.

### Fractionator: neuronal number estimate

The primary somatosensory barrel cortex was identified based on morphological and histological boundaries: the molecular layer I on the dorsal surface, the distinct changes in neuronal size and density between layers, and the reduction in layer IV thickness to indicate the lateral extents of the cortical barrel fields (Supplementary Figure 1). Every sixth section containing the somatosensory barrel cortex was selected to obtain a sample in a systematic uniform random manner (section-sampling fraction; $ssf = 0.166$), yielding 8–10 sections per brain. The first of these sections was randomly selected. In the sampled sections, an optical disector counting frame was employed for counting and measuring neuronal nuclei at predetermined regular $x$, $y$ intervals (Gundersen 1977). Inclusion and exclusion counting criteria were followed by a blinded observer who recorded counts only when a single neuronal nucleolus was brought into focus within the disector frame (Sterio 1984). Healthy neurons were distinguished from other objects such as astrocytes and microglia based on the presence of a distinguishable nuclear membrane, unstained nucleus and dense nucleolus within the cell in question, in accordance with criteria previously used in stereological studies to identify neurons (West 1993; Witgen et al. 2005; Lifshitz et al. 2007). Unhealthy neurons (dystrophic or multiple nuclei and/or inconsistent nuclear membranes) were not quantified. Because the area ($a$) of the counting frame was known relative to the regular stage-stepping intervals over the section, one can calculate the area sampling fraction ($asf$) = $a$ (frame)/$a$ ($x$, $y$ step) as 0.0744, 0.1246, and 0.0997 for layers II/III, IV and V, respectively. The height ($h$ = 25–29 μm) of the optical disector was equivalent to the thickness of the section ($t = 27.30 \pm 0.67$ μm). With these parameters, the estimated number of neurons ($N$) followed from the formula $N = \sum Q^- \times t/h \times 1/\text{asf} \times 1/\text{ssf}$, where $\sum Q^-$ was the number of neurons counted.

To analyze the sampling scheme reliability, for every animal, coefficient of error (CE) was calculated using Matheron's quadratic approximation (Gundersen and Jensen 1987) and by considering the ''nugget effect'' (West et al. 1996) to reflect the variance introduced by the sampling of tissue sections (Table 1). All samplings were conducted using an Olympus BH-2 microscope with an ASI automatic stage (Olympus, USA), using a 100×, 1.3 numerical aperture oil immersion objective (Olympus, Japan). A mounted video camera (QImaging, BC, Canada), and microcator (Heidenhaim, Deerfield, IL) were used in conjunction with Bioquant Life Science Image Analysis software package (Bioquant, Nashville, TN) which included Stereology and Topography plugins.

**Table 1** Stereological parameters and estimated total number of neurons in the cortical layers of the primary somatosensory barrel fields of sham and brain-injured rats

| | Layer II/III | Layer IV | Layer V |
|---|---|---|---|
| $\sum Q^- \pm$ SEM | | | |
| Sham | 96 ± 7 | 104 ± 18 | 96 ± 14 |
| 1 day FPI | 79 ± 7 | 118 ± 17 | 88 ± 11 |
| 7 day FPI | 53 ± 6 | 61 ± 12 | 64 ± 3 |
| 28 day FPI | 90 ± 7 | 119 ± 14 | 106 ± 10 |
| Est. num ± SEM | | | |
| Sham | 7,744 ± 579 | 4,985 ± 867 | 5,791 ± 835 |
| 1 day FPI | 6,353 ± 560 | 5,696 ± 838 | 5,310 ± 669 |
| 7 day FPI | 4,243 ± 444 | 2,957 ± 564 | 3,827 ± 202 |
| 28 day FPI | 7,276 ± 567 | 5,713 ± 668 | 6,366 ± 619 |
| Mean (CE) | | | |
| Sham | 0.122 | 0.113 | 0.106 |
| 1 day FPI | 0.120 | 0.107 | 0.114 |
| 7 day FPI | 0.153 | 0.164 | 0.136 |
| 28 day FPI | 0.108 | 0.099 | 0.105 |
| OCV | | | |
| Sham | 0.150 | 0.348 | 0.288 |
| 1 day FPI | 0.197 | 0.329 | 0.282 |
| 7 day FPI | 0.234 | 0.427 | 0.118 |
| 28 day FPI | 0.174 | 0.262 | 0.218 |
| Percent reduction from sham | | | |
| 1 day FPI | 18.0% | −14.3% | 8.3% |
| 7 day FPI | 45.2% | 40.7% | 33.9% |
| 28 day FPI | 6.0% | −14.6% | −9.9% |

Mean ± standard error of the mean

*FPI* fluid percussion injury, $\sum Q^-$ number of neurons counted, *CE* coefficient of error, *OCV* observed coefficient of variation

### Vertical nucleator: neuronal nuclear volume estimate

Unbiased object volume ($\mu m^3$) can be estimated using the vertical nucleator stereological probe. As employed in the present communication, the vertical nucleator provided assumption-free estimates of mean neuronal nuclear volume in systematically sampled neurons within distinct layers of somatosensory barrel cortex (Gundersen 1988; Lifshitz et al. 2007). Two randomly oriented length cubed rulers ($L^3$) extend from a central point of the object (nucleolus) and are measured at the intersection with the nuclear membrane (Gundersen 1988).

The vertical nucleator probe was used to estimate unbiased object volume within the somatosensory barrel cortex, using tissue sectioned in the coronal plane, in which neurons are randomly oriented. When the neuronal nucleolus was in focus, the nucleator was applied. Two randomly oriented, perpendicular length cubed rulers ($L^3$) extend from a central point in the nucleolus and the intersections of the rulers with the nuclear boundary are marked. Measurements of nuclear volume, rather than somatic volume, provide clear and objective boundaries of the nuclear membrane surrounding the unstained nucleus. The BioQuant software package calculated the neuronal volume based on the length cubed rulers. The nucleator was applied to an average of 88.4 ± 4.1 neurons per cortical layer (range = 27–173). In addition to the quantitative measurements of the mean of the neuronal population, individual neuron measurements for each animal were separated across thirteen 25 $\mu m^3$ bins to establish population distribution histograms.

### Cavalieri principle: regional volume estimate

Estimates of regional volume were obtained by the Cavalieri method, based on systematically random point counting. The volume of the primary somatosensory barrel cortex was estimated by counting the number of unique points along a systematically random grid established in pilot studies for each cortical layer (layer II/III, 110 μm × 110 μm; layer IV, 85 μm × 85 μm; layer V, 95 μm × 95 μm) across the outlined region that fell within the region of interest. Each included point represents a known area, such that the sum of the number of points lying within the region multiplied by the corresponding area (layer II/III, 12,100 $\mu m^2$; layer IV, 7,225 $\mu m^2$; layer V, 9,025 $\mu m^2$) multiplied by the represented thickness (30 μm × 6 sections) yields an estimate of the somatosensory barrel cortex volume for each animal. The coefficient of error (CE) was calculated for each animal, such that the mean CEs of the individual estimates of somatosensory barrel cortex volume were 0.12, 0.13, 0.12, and 0.13 for sham, 1 day FPI, 7 days FPI, and 28 days FPI, respectively.

#### Statistical tests

Data for each cortical segment or layer were treated as separate datasets and analyzed separately. Means for quantification of the argyrophilic reaction product, neuronal nuclear volume, neuronal number, regional volume and neuronal density were analyzed by a one-way ANOVA across post-injury time points, followed by Student Neumann–Keuls post-test to determine an injury effect. Neuronal nuclear size distributions were analyzed by two-way ANOVA between time post-injury and the bin size. Statistical tests were considered significant at the $p < 0.05$ confidence level. Data are presented as mean ± standard error of the mean.

## Results

#### Primary somatosensory cortex gross histopathology

Previous studies have demonstrated acute membrane perturbation, perisomatic axotomy and protease activation across the thalamus and somatosensory cortex after identical midline fluid percussion brain injury (Singleton and Povlishock 2004; Kelley et al. 2006; McGinn et al. 2009). The mechanical forces of this injury continue to produce no overt hemorrhage, edema, contusion or cavitation, as observed at 1 day, 7 days and 28 days post-injury in primary somatosensory barrel cortex (Fig. 1). At a macroscopic level, gross histopathology in the somatosensory barrel cortex is unremarkable between uninjured sham and injured brains, maintaining cytological distinction between cortical layers at least up to 1-month post-injury. Cortical thickness measurements were not evaluated.

#### Argyrophilic reaction product identified neurodegeneration

Tissue was stained by the de Olmos amino cupric silver technique over the post-injury time course to identify argyrophilic reaction product, commonly interpreted as neurodegeneration, within the primary somatosensory cortex. As expected, no appreciable argyrophilic reaction product was observed in uninjured sham brain (Fig. 2a). At 1 day post-injury, argyrophilic reaction product accumulation was present in the superficial segment across the expanse of primary somatosensory cortex, with selective labeling of the cortical barrels (Fig. 2b). By 7 days post-injury, argyrophilic reaction product accumulation progressed to middle and deeper cortical segments, including

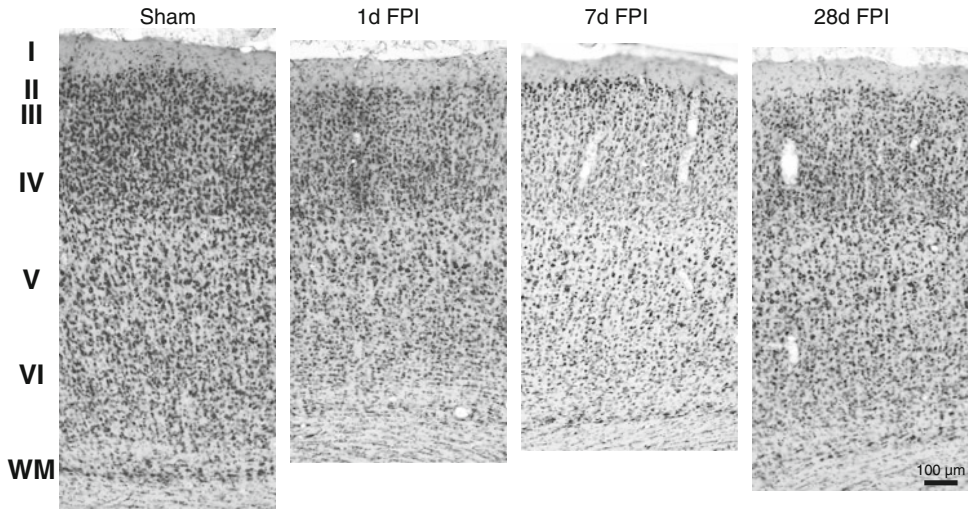


**Fig. 1** Diffuse brain injury modeled by midline fluid percussion injury (FPI) occurs in the absence of overt hemorrhage, edema or cavitation. Distinct cortical layers based on cytology remain preserved in primary somatosensory barrel cortex (layers I–VI) over time post-injury. Cortical thickness was not measured. *Scale Bar* = 100 µm

subcortical white matter (Fig. 2c). By 28 days post-injury, argyrophilic reaction product accumulation is preferentially found within the inter-barrel septa of layer IV, middle and deeper cortical segments and subcortical white matter (Fig. 2d).

Since neurodegeneration progressed deeper through the cortex over time post-injury, further analyses divided the cortex into thirds to evaluate superficial, middle and deep segments of the cortex. Cytoarchitectural layers could not be delineated clearly. At 1 day post-injury, reaction product was restricted to superficial and middle segments of the cortex (Fig. 3a). The argyrophilic reaction product was primarily found in thin processes (axons and/or dendrites) in various orientations. Light microscopy was insufficient

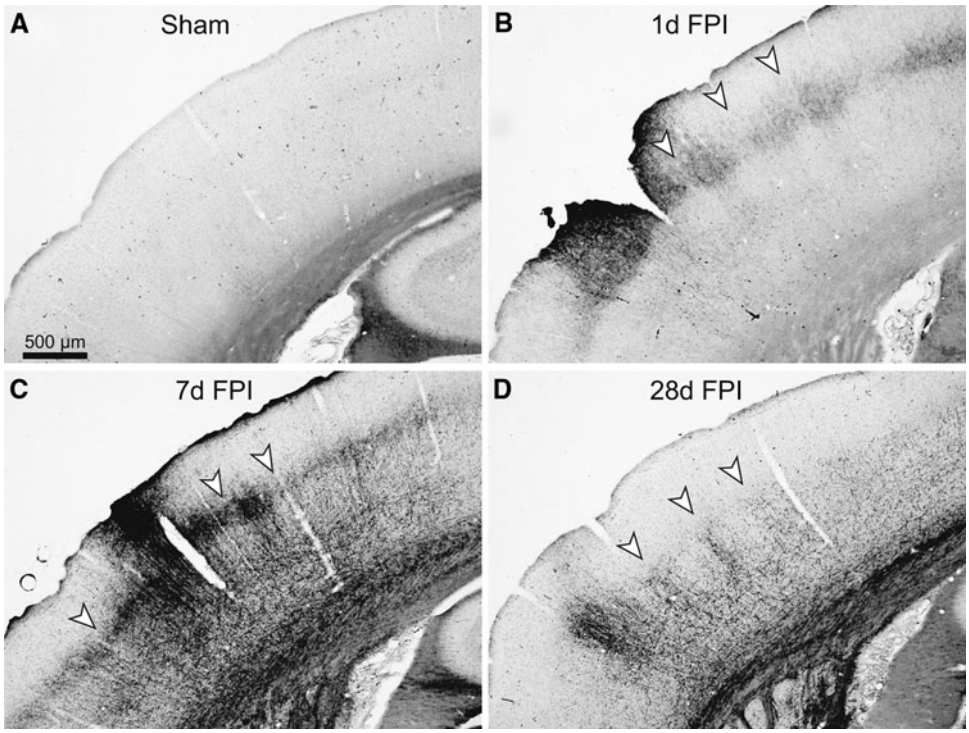


**Fig. 2** Post-traumatic time course of argyrophilic reaction product in the primary somatosensory barrel cortex as revealed by the de Olmos silver staining technique in uninjured sham (**a**) and at 1 day (**b**), 7 days (**c**) and 28 days (**d**) after moderate midline fluid percussion brain injury. Uninjured sham brain was absent of argyrophilic reaction product. At 1 day post-injury, argyrophilic reaction product was localized to the superficial segment of the cortex, particularly within the cortex barrels (*between white arrowheads*). At 7 days post-injury, argyrophilic reaction product progressed to the middle segment of the cortex and remained preferentially in the cortical barrels. By 28 days post-injury, argyrophilic reaction product appears absent in the superficial segment and diffuse across the middle and deeper segments of the cortex. By this time, staining encompasses the inter-barrel septa (*white arrowheads*)

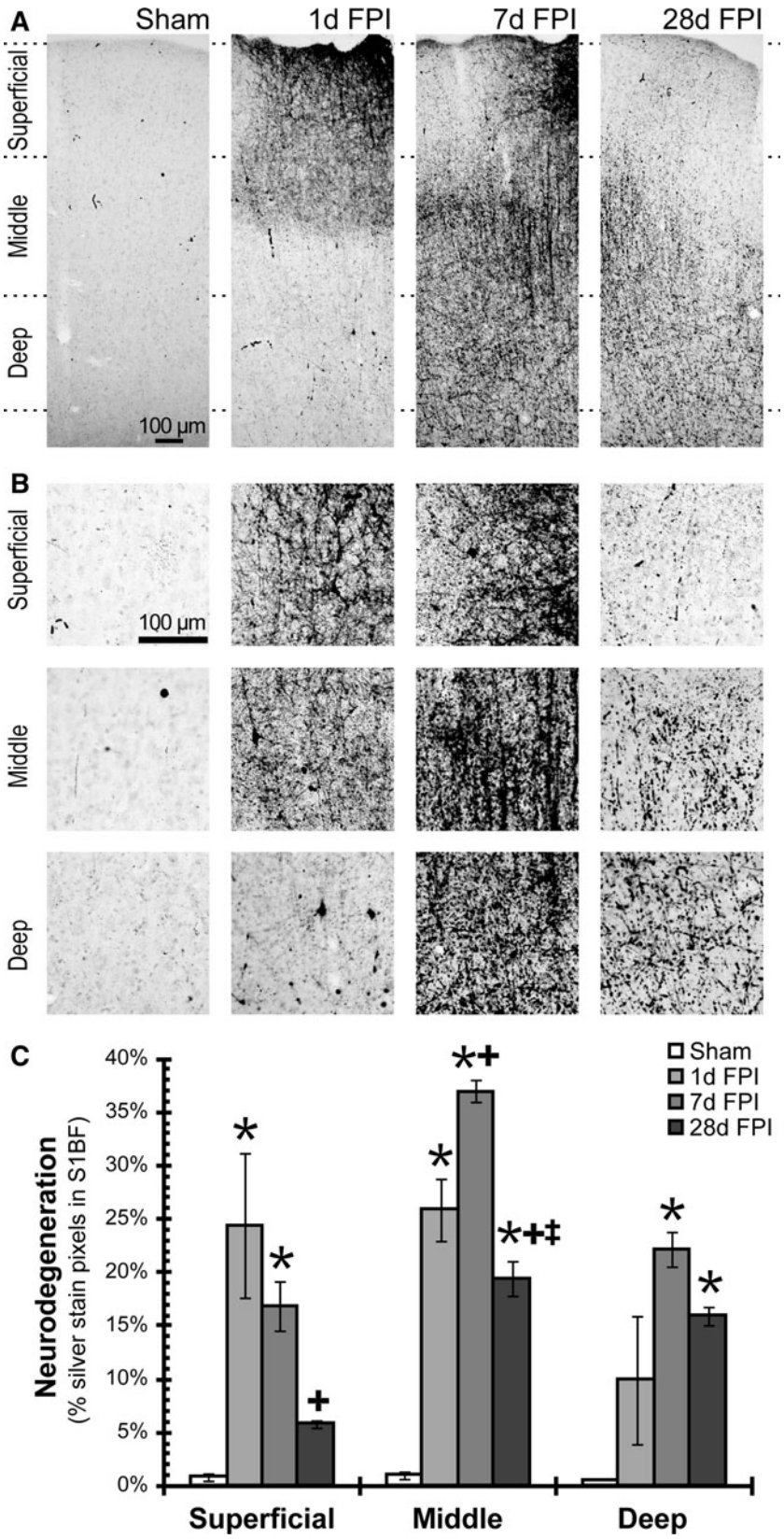


**Fig. 3** Argyrophilic reaction product progresses through the cortex over time post-injury. **a** Photomicrographs of primary somatosensory barrel cortex (S1BF) processed by the de Olmos silver staining technique show no appreciable accumulation in uninjured sham brain and indication of degeneration that progresses to deeper segments of the cortex with time post-injury. The cortical mantle has been divided by thirds into superficial, middle and deep segments. **b** Higher power photomicrographs of each segment of S1BF cortex show the progression through deeper segments and dense argyrophilic reaction product in neuronal processes, which likely include axons, dendrites and synaptic terminals. Infrequent stained somata are present, primarily at 1 day post-injury in the middle and deep segments. **c** Argyrophilic reaction product was quantified as a percent of silver stained pixels in each cortical segment (pixel quantification; see "Materials and methods"). As visualized, degeneration in the superficial segment increased significantly at 1 day after fluid percussion injury (FPI) and subsided over 28 days. In the middle segment, degeneration continued to increase over 1 and 7 days post-injury and remained elevated at 28 days post-injury compared to uninjured sham. In the deep segment, a delayed increase in degeneration was observed at 7 and 28 days post-injury compared to sham. (mean ± SEM; $^{*}p < 0.05$ compared to sham; $^{+}p < 0.05$ compared to 1 day FPI; $^{\ddagger}p < 0.05$ compared to 7 days FPI)

to delineate between processes cut in cross section and synaptic terminals. Infrequent reactive cell bodies were observed, as indicated in both superficial and middle segments at 1 day post-injury (Fig. 3b). At 7 days post-injury, qualitatively similar staining to 1 day post-injury was observed, but primarily in middle and deep segments of the cortex. Throughout the middle segment, dense reactive processes perpendicular to the pial surface were observed. By 28 days post-injury, much of the argyrophilic reaction product was restricted to middle and deep cortical segments, with an apparent lower density of reactive processes.

Pixel quantification revealed significant argyrophilic reaction product in primary somatosensory cortex of brain-injured animals over the observed 1-month post-injury time course (Fig. 3c). In the superficial segment of the cortex, significant argyrophilic reaction product was evident at 1 day and 7 days post-injury compared to uninjured sham and returned to sham levels by 28 days post-injury [$F(3, 8) = 8.823$, $p = 0.0064$]. In the middle segment of the cortex, significant argyrophilic reaction product was evident at 1 day post-injury compared to sham, which further increased significantly at 7 days post-injury compared to sham and 1 day brain-injured samples; by 28 days post-injury, argyrophilic reaction product remained significantly elevated above uninjured sham, but reduced compared to 1 and 7 days post-injury [$F(3, 8) = 74.601$, $p < 0.0001$]. In the deep segment of the cortex, significant argyrophilic reaction product was evident at 7 and 28 days post-injury compared to uninjured sham, without significant changes at 1 day post-injury [$F(3, 8) = 8.717$, $p = 0.0067$]. Therefore, degeneration of neuronal processes (which include axons, dendrites, cell bodies and likely terminals) within the primary somatosensory barrel field progresses from superficial to deep segments and from within the barrels to the septa over time post-injury.

## Injury-induced atrophy of neuronal nuclear volume

The preserved cytoarchitecture of the somatosensory cortex allowed a layer specific analysis of neuronal nuclear volumes over time post-injury. As expected, the largest neurons were the motor neurons of layer V of somatosensory cortex. Using the vertical nucleator, significant neuronal nuclear atrophy was evident in brain-injured rats at 7 days after diffuse brain injury across all cortical layers [layer II/III: $F(3, 14) = 4.289$, $p = 0.024$; layer IV: $F(3, 14) = 4.926$, $p = 0.015$; layer V: $F(3, 14) = 7.956$, $p = 0.002$] compared to sham (Fig. 4). In layer V, neuronal nuclear volumes were significantly smaller than sham at all post-injury time points. The atrophy in neuronal nuclear volume at 28 days after brain injury compared to sham in cortical layers II/III and IV was not significant.

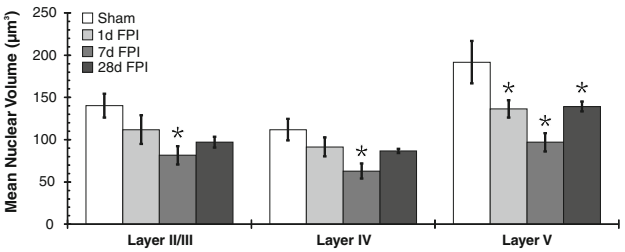


**Fig. 4** Brain injury-induced atrophy of neuronal nuclear volume was estimated using the nucleator probe. Fluid percussion injury (FPI) results in a significant reduction in mean neuronal nuclear volume in all cortical layers at 7 days post-injury compared to sham ($*p < 0.05$). Injury-induced neuronal atrophy is evident in Layer V at all post-injury time points compared to sham ($*p < 0.05$). Values are mean ± SEM

## Injury-induced shift in neuronal nuclear size distribution across cortical layers in the primary somatosensory barrel field

Neuronal nuclear measurements were pooled across sections within animals, separated into 25 $\mu m^3$ bins and averaged across animals within a given group (Fig. 5). After brain injury, the nuclear size distributions indicate shifts toward smaller nuclear volumes, as indicated by significantly fewer neurons larger than the sham mean (grey vertical lines in Fig. 5) and/or significantly more neurons smaller than the sham mean. Significant neuronal atrophy was observed in all three cortical layers, over the post-injury time course examined, as identified by two-way ANOVAs between time post-injury and the bin size [layer II/III: $F(36, 182) = 3.745$, $p < 0.001$; layer IV: $F(36, 182) = 2.847$, $p < 0.001$; layer V: $F(36, 182) = 3.77$, $p < 0.001$]. Taken together, these data support consistent neuronal atrophy in primary somatosensory cortex across all post-injury time points.

## Transient reduction of healthy neuron number after brain injury

Stereological procedures were employed to quantify the number of healthy neurons (unstained nucleus with a condensed nucleolus) remaining in the primary somatosensory barrel cortex after diffuse brain injury. The number of healthy neurons in S1BF cortical layers II/III, IV and V were estimated for sham, 1 day FPI, 7 day FPI and 28 days FPI (Fig. 6a, Table 1). Statistically significant reductions in estimated total neuron number at 7 days post-injury were achieved in cortical layer II/III [$F(3, 14) = 8.376$; $p = 0.002$] and layer V [$F(3, 14) = 3.465$; $p = 0.045$] compared to uninjured sham or other time points. Neuron numbers in layer IV were not significantly different between uninjured and brain-injured animals [$F(3, 14) = 3.277$; $p = 0.0528$]. The sampling procedures employed to estimate neuronal number are sufficient, as the

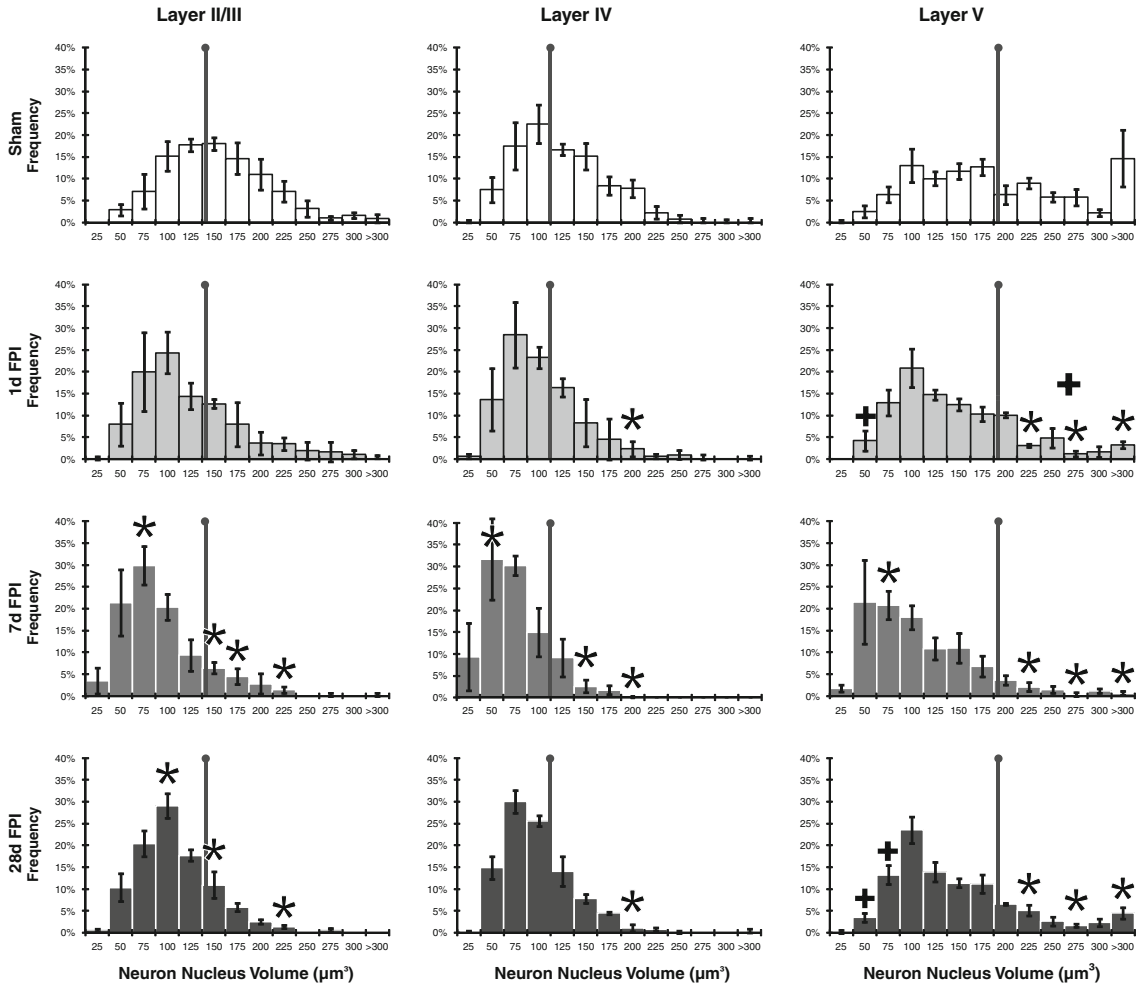


**Fig. 5** Injury-induced shifts in neuronal nuclear size distribution across cortical layers in the primary somatosensory barrel fields. Nucleator measurements were pooled across sections and binned by size. The frequency of each volume measurement is plotted for sham and fluid percussion injured (FPI) animals. After brain injury, the nuclear size distributions show significant shifts toward smaller volumes (mean ± SEM; * and $^{+}p < 0.05$ compared to sham and 7 days FPI for each size bin, respectively). Neuronal populations from brain-injured animals show fewer neurons that are larger than the mean of the sham group (*grey vertical line*). Additionally, for brain-injured animals, there are more neurons in the bins smaller than the mean of the sham group

coefficient of error (CE), representing the intra-animal variability associated with the sampling procedures, ranged from 0.10 to 0.16 in all animals (Table 1) (Gundersen and Jensen 1987; West et al. 1991). The coefficient of variation (CV), representing inter-animal biological variability, indicates that biology, rather than the sampling procedures, contributes to the variability in the data (Table 1).

Estimates of regional volume were obtained using the Cavalieri principle to enable calculations of neuronal density. No significant differences in the volume of the primary somatosensory cortex layers II/III [$F(3, 14) = 1.299$; $p = 0.314$], layer IV [$F(3, 14) = 0.502$; $p = 0.687$], or layer V [$F(3, 14) = 0.472$; $p = 0.706$] were detected (Fig. 6b). In calculating neuronal density (number of neurons/regional volume), all the cortical layers of brain-injured rats at 7 days post-injury had significantly lower neuronal densities than uninjured and/or other post-injury time points [layer II/III: $F(3, 14) = 8.452$; $p = 0.002$; layer IV: $F(3, 14) = 5.140$; $p = 0.013$; layer V: $F(3, 14) = 8.981$; $p = 0.001$; Fig. 6c]. Neuronal densities at 28 days post-injury were not significantly different from values in uninjured animals. Injury-induced reductions in neuronal density are not related to differential tissue shrinkage since uniform tissue shrinkage was observed in all groups (Lifshitz et al. 2007).

Therefore, the composition of healthy neurons within the primary somatosensory cortex of rats subjected to diffuse brain injury changes transiently over the observed 1-month post-injury time course.

## Discussion

Neuropathological evaluation of the diffuse-injured brain demonstrated neurodegeneration over 1-month post-injury

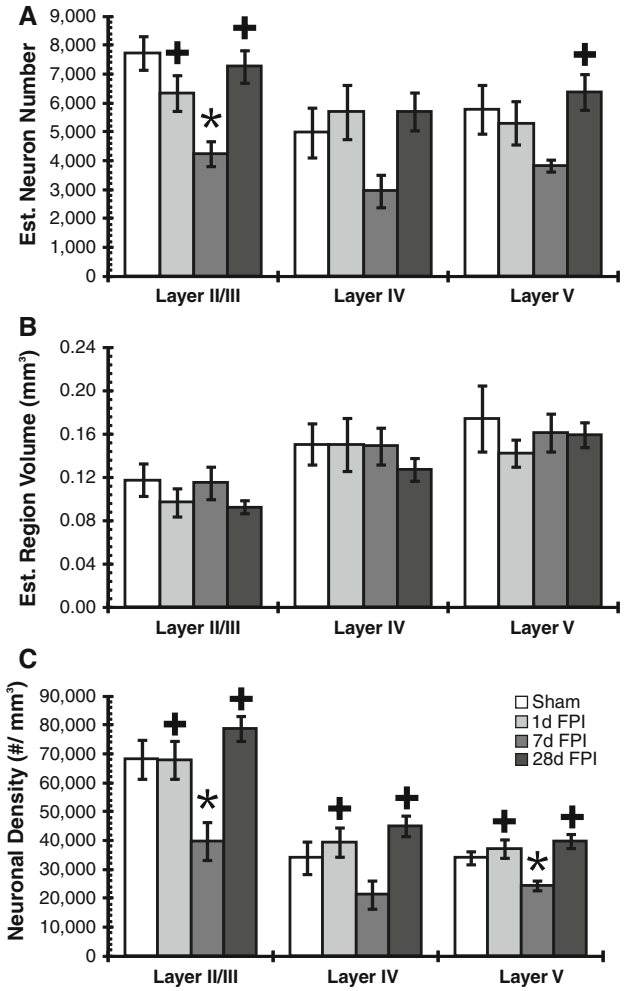


**Fig. 6** Stereological quantification in the S1BF using the fractionator and Cavalieri principles to estimate neuronal number and regional volume, respectively. **a** At 7 days post-injury, the number of neurons in Layer II/III was significantly less than sham and other post-injury time points. Neuronal number is significantly different between 7 and 28 days post-injury in layer V. **b** No injury-related changes in regional volume were detected. Estimates of regional volume were obtained by the Cavalieri method, based on systematically random point counting. **c** Neuronal density calculations indicate significant injury-related reductions at 7 days post-injury compared to sham and other post-injury time points. (mean ± SEM; $*p < 0.05$ compared to sham; $^{+}p < 0.05$ compared to 7 days FPI)

in the primary somatosensory barrel cortex (S1BF), as an additional component of the somatosensory whisker barrel circuit that also suffers pathology in the thalamic relays (Lifshitz et al. 2007). Neuropathological evaluation included qualitative and quantitative evaluation of argyrophilic reaction and stereological quantification of neuronal nuclear volume, neuronal number and neuronal density; together these define neurodegeneration in the present communication. By 1-month post-injury, the density of healthy neuron number has returned to uninjured sham levels, but evidence of ongoing argyrophilic reaction and neuronal atrophy persist. Ongoing neurodegenerative responses to diffuse brain injury likely disrupt the connectivity of this functionally relevant and anatomically distinct circuit, giving rise to late onset, persistent sensory sensitivity to whisker stimulation (McNamara et al. 2010). Similar circuit disruption and consequent reorganization may underlie the spectrum of post-traumatic morbidities reported for post-concussion syndrome (McAllister 1992; Nakamura et al. 2009). These results are intriguing, given that diffuse brain injury is uncomplicated by contusion and occurs in the absence of overt hemorrhage or edema (McGinn et al. 2009).

We report cytoarchitecturally distinct argyrophilic reaction product accumulation that progressed into deeper cortical segments and spread within the cortical barrels over time post-injury. The impact associated with the fluid percussion injury affects widespread cortical and subcortical regions, but argyrophilic reaction product preferentially localized to the S1BF cortical domains. Separately, we are investigating the relationship between the injury forces and the structure of the rat skull to explain this susceptibility. In these areas of reaction product accumulation, neurons are likely undergoing degenerative processes, including dendritic reorganization, synaptic sprouting and/or frank degeneration (Beltramino et al. 1993; Switzer 2000). The argyrophilic reaction was found infrequently in neuronal somata and primarily in thin processes (axons and/or dendrites), which may include synaptic terminals. Future ultrastructural analyses will determine the extent of axolemmal, dendritic, somatic and terminal degeneration. The argyrophilic reaction across S1BF may include or lead to the observed persistent neuronal atrophy, which then explains the transient reduction in healthy neuronal number as atrophic neurons no longer meet strict inclusion counting criteria. These changes may occur in the presence or absence of axotomy and not necessarily result in cell death (Singleton et al. 2002; Lifshitz et al. 2007), despite evidence for TUNEL positive staining (Singleton et al. 2002), membrane perturbation (Kelley et al. 2006), and protease activation (McGinn et al. 2009). Efforts to reestablish homeostatic balance would promote cellular repair (i.e. receptor or ion channel composition), accounting for the restoration of neuronal number and volume at later time points (Turrigiano and Nelson 2004; Turrigiano 2008).

The current communication evaluated neuropathology in S1BF up to 28 days after a moderate diffuse brain injury. The degeneration previously observed in the thalamic relay to S1BF predicted pathology in S1BF (Lifshitz et al. 2007). The studies were terminated at 28 days, because behavioral morbidity associated with sensory sensitivity to whisker stimulation becomes established within that time frame, neither worsening nor improving over 56 days post-injury

(McNamara et al. 2010). The transient reduction in number and atrophy of neuronal nuclei in the cortex may be associated with the post-injury argyrophilic reaction (1–7 days post-injury) followed by injury-responsive regenerative changes (7–28 days post-injury). Neuropathology likely occurs in the cortico-thalamic direction, given that reductions in neuronal number occur earlier in the cortex than in the thalamus (Lifshitz et al. 2007). Tracer-labeled circuits would verify injury-induced remodeling between thalamic and cortical domains, but not necessarily the directionality. In addition, similar reductions in neuronal number and subsequent recovery have been reported in the contralateral hippocampus after lateral fluid percussion brain injury (Tran et al. 2006). Unchanged regional volumes over time post-injury suggest limited net cellular edema, but possibly a compensatory vascular or glial swelling to compensate for the observed neuronal nuclear atrophy in the cortex. Thus, the neurodegeneration of diffuse brain injury manifests as argyrophilic reaction and atrophic change, as supported by our prior data in the ventral basal complex (Lifshitz et al. 2007) and lateral vestibular nucleus (Hosseini and Lifshitz 2009).

The progression of the argyrophilic reaction does not necessarily indicate irreversible damage, but rather cyto-architectural responses to disease, injury or signaling. A century of lesion studies have employed variations of the silver histochemical technique to explore long-range connectivity. Similarly, argyrophilic reaction product accumulation identified local neurodegeneration at the cortical impact site and long-range degeneration in the contralateral hemisphere after focal brain injury (Hall et al. 2008). The silver technique identified both focal and diffuse regions of degeneration after the diffuse brain injury employed in the present manuscript. Since frank degeneration of parenchyma was not observed, the argyrophilic reaction likely identifies structural organization. Similarly, pharmacological inhibition of NMDA receptors by systemic MK-801 administration results in argyrophilic reaction product in various cortical and hippocampal regions (de Olmos et al. 2009). This transient loss of synaptic inputs leads to morphological changes that outlast the acute induction of immediate early gene expression (cFos, FosB) (de Olmos et al. 2009). Our results support the conclusion that morpho-functional alterations compensate for circuit inhibition, whether initiated by pharmacological inhibition or mechanical trauma.

Direct mechanical forces may render superficial layer II/III the most vulnerable. Yet, progressive neurodegeneration into deeper cortical layers likely reflect consequences of axonal injury, axotomy and deafferentation (Steward 1989; Singleton et al. 2002). Diffuse axonal injury along white matter tracts at grey–white interfaces may directly disrupt thalamocortical and corticothalamic projections (Smith et al. 1997; Meythaler et al. 2001), initiating neuronal change in the middle and deep layer IV and V. The time-dependent reductions in healthy neuron number and nuclear volume support an acute degenerative phase (1–7 days post-injury). An ensuing regenerative phase is inferred from the partial restoration of healthy neuron number and volume by 28 days post-injury. More detailed spatial and temporal analyses could assess individual cortical barrels to delineate the progression of argyrophilic reaction from within the barrel and septal regions. In human autopsy samples, degeneration and partial restoration of diffuse-injured tissue may underlie the cell loss and shrinkage across cortical domains (Maxwell et al. 2010).

As a surrogate marker of neuronal somatic volume, neuronal nuclear volumes via shrinkage or expansion have been shown to reflect cellular atrophy or hypertrophy, respectively, in neurodegenerative disease (Finch 1993; Sa et al. 2000; Bothwell et al. 2001). Neuronal atrophy over the first week post-injury suggests that degenerative events may limit neurotrophic signaling necessary to maintain cellular homeostasis (Rich et al. 1989; Sofroniew et al. 1993). Similarly, excitotoxic lesions of basal forebrain cholinergic targets leave neurons atrophic in the absence of target-derived trophic support (Sofroniew et al. 1993). The restoration of healthy neuron size and number suggests a reinstatement of trophic support, from either autocrine or paracrine sources (Rich et al. 1984; Gold et al. 1991). The possibility remains that the reorganization of brain-injured circuits provides synaptic sources of trophic factors. Whether the reinstatement of neuronal number and volumes are contingent upon neuroplastic responses for circuit reorganization remain to be shown (Hall and Lifshitz 2010).

The results implicate a temporal series of degenerative and reorganizational changes after diffuse brain injury that may serve as potential therapeutic targets. Acute treatments could focus on neuronal health through energy substrates or trophic factors (Saatman et al. 1997; Royo et al. 2007; Prins 2008). Delayed treatments could target the structural reorganization by encouraging activity-dependent plasticity or impairing synaptogenesis after unregulated plasticity (Kleim et al. 2003; Feldman and Brecht 2005; Gogolla et al. 2007). Effective therapies would mitigate the cellular neuropathology in the somatosensory cortex (current communication), thalamic relay for whisker sensation (Lifshitz et al. 2007), broad functional activation of the whisker circuit (Hall and Lifshitz 2010) and behavioral allodynia to whisker stimulation (McNamara et al. 2010).

In summary, we postulate that circuit reorganization, initiated by degenerative events and concluding with plastic events, is responsible for the functional and behavioral consequences of diffuse brain injury. Here, we showed neurodegeneration in the somatosensory cortex

over 1 month after diffuse brain injury. Over time, the numbers of healthy neurons and their nuclear volumes are restored as degenerative change progresses deeper into the cortex and outside the cortical barrels. These neuropathological events in the cortex indicate degenerative and regenerative processes that may interfere with neural circuit function, explaining the behavioral morbidity elicited by whisker stimulation in the diffuse brain-injured rodent (McNamara et al. 2010). Similar post-traumatic cellular events in man may disrupt neural circuits, underlying the spectrum and intensities of post-traumatic morbidities (McAllister 1992).

**Acknowledgments** We are grateful to Dr. John T. Povlishock, Ms. C. Lynn Davis and Ms. Sue Walker for support and assistance in generating the tissue for stereological analysis. We thank the reviewers for constructive criticisms that improved the manuscript. This work was supported, in part, by the National Institutes of Health research grant (R01 NS065052) and core facility grant (P30 NS051220) and the Kentucky Spinal Cord and Head Injury Research Trust (7-11).

## References

Beltramino CA, de Olmos JS, Gallyas F, Heimer L, Zaborszky L (1993) Silver staining as a tool for neurotoxic assessment. NIDA Res Monogr 136:101–126

Biasca N, Maxwell WL (2007) Minor traumatic brain injury in sports: a review in order to prevent neurological sequelae. Prog Brain Res 161:263–291

Bohnen N, Twijnstra A, Wijnen G, Jolles J (1991) Tolerance for light and sound of patients with persistent post-concussional symptoms 6 months after mild head injury. J Neurol 238:443–446

Bothwell S, Meredith GE, Phillips J, Staunton H, Doherty C, Grigorenko E, Glazier S, Deadwyler SA, O'Donovan CA, Farrell M (2001) Neuronal hypertrophy in the neocortex of patients with temporal lobe epilepsy. J Neurosci 21:4789–4800

Christodoulou C, DeLuca J, Ricker JH, Madigan NK, Bly BM, Lange G, Kalnin AJ, Liu WC, Steffener J, Diamond BJ, Ni AC (2001) Functional magnetic resonance imaging of working memory impairment after traumatic brain injury. J Neurol Neurosurg Psychiatry 71:161–168

de Olmos JS, Beltramino CA, de Olmos de Lorenzo S (1994) Use of an amino-cupric-silver technique for the detection of early and semiacute neuronal degeneration caused by neurotoxicants, hypoxia, and physical trauma. Neurotoxicol Teratol 16:545–561

de Olmos S, Bender C, de Olmos JS, Lorenzo A (2009) Neurodegeneration and prolonged immediate early gene expression throughout cortical areas of the rat brain following acute administration of dizocilpine. Neuroscience 164:1347–1359

Feldman DE, Brecht M (2005) Map plasticity in somatosensory cortex. Science 310:810–815

Finch CE (1993) Neuron atrophy during aging: programmed or sporadic? Trends Neurosci 16:104–110

Giaume C, Maravall M, Welker E, Bonvento G (2009) The barrel cortex as a model to study dynamic neuroglial interaction. Neuroscientist 15:351–366

Glassman RB (1994) Behavioral specializations of si and sii cortex: A comparative examination of the neural logic of touch in rats, cats, and other mammals. Exp Neurol 125:134–141

Gogolla N, Galimberti I, Caroni P (2007) Structural plasticity of axon terminals in the adult. Curr Opin Neurobiol 17:516–524

Gold BG, Mobley WC, Matheson SF (1991) Regulation of axonal caliber, neurofilament content, and nuclear localization in mature sensory neurons by nerve growth factor. J Neurosci 11:943–955

Greer JE, McGinn MJ, Povlishock JT (2011) Diffuse traumatic axonal injury in the mouse induces atrophy, c-jun activation, and axonal outgrowth in the axotomized neuronal population. J Neurosci 31:5089–5105

Gundersen HJG (1977) Notes on the estimation of the numerical density of arbitrary profiles: the edge effect. J Microsc 147:219–223

Gundersen HJG (1988) The nucleator. J Microsc 151:3–21

Gundersen HJG, Jensen EB (1987) The efficiency of systematic sampling in stereology and its prediction. J Microsc 147:229–263

Hall KD, Lifshitz J (2010) Diffuse traumatic brain injury initially attenuates and later expands activation of the rat somatosensory whisker circuit concomitant with neuroplastic responses. Brain Res 1323:161–173

Hall ED, Bryant YD, Cho W, Sullivan PG (2008) Evolution of post-traumatic neurodegeneration after controlled cortical impact traumatic brain injury in mice and rats as assessed by the de olmos silver and fluorojade staining methods. J Neurotrauma 25:235–247

Hosseini AH, Lifshitz J (2009) Brain injury forces of moderate magnitude elicit the fencing response. Med Sci Sports Exerc 41:1687–1697

Kelley BJ, Farkas O, Lifshitz J, Povlishock JT (2006) Traumatic axonal injury in the perisomatic domain triggers ultrarapid secondary axotomy and wallerian degeneration. Exp Neurol 198:350–360

Kleim JA, Jones TA, Schallert T (2003) Motor enrichment and the induction of plasticity before or after brain injury. Neurochem Res 28:1757–1769

Langlois JA, Rutland-Brown W, Thomas KE (2004) Traumatic brain injury in the united states: emergency department visits, hospitalizations, and deaths. Centers for Disease Control and Prevention, National Center for Injury Prevention and Control, Atlanta

Levine B, Cabeza R, McIntosh AR, Black SE, Grady CL, Stuss DT (2002) Functional reorganisation of memory after traumatic brain injury: a study with h(2)(15)0 positron emission tomography. J Neurol Neurosurg Psychiatry 73:173–181

Lifshitz J (2008) Fluid percussion injury. In: Chen J, Xu Z, Xu XM, Zhang J (eds) Animal models of acute neurological injuries. The Humana Press, Inc, Totowa, NJ

Lifshitz J, Kelley BJ, Povlishock JT (2007) Perisomatic thalamic axotomy after diffuse traumatic brain injury is associated with atrophy rather than cell death. J Neuropathol Exp Neurol 66:218–229

Maxwell WL, Pennington K, MacKinnon MA, Smith DH, McIntosh TK, Wilson JT, Graham DI (2004) Differential responses in three thalamic nuclei in moderately disabled, severely disabled and vegetative patients after blunt head injury. Brain 127:2470–2478

Maxwell WL, MacKinnon MA, Stewart JE, Graham DI (2010) Stereology of cerebral cortex after traumatic brain injury matched to the glasgow outcome score. Brain 133:139–160

McAllister TW (1992) Neuropsychiatric sequelae of head injuries. Psychiatr Clin North Am 15:395–413

McGinn MJ, Kelley BJ, Akinyi L, Oli MW, Liu MC, Hayes RL, Wang KK, Povlishock JT (2009) Biochemical, structural, and biomarker evidence for calpain-mediated cytoskeletal change after diffuse brain injury uncomplicated by contusion. J Neuropathol Exp Neurol 68:241–249

McNamara KC, Lisembee AM, Lifshitz J (2010) The whisker nuisance task identifies a late-onset, persistent sensory sensitivity in diffuse brain-injured rats. J Neurotrauma 27:695–706

Meythaler JM, Peduzzi JD, Eleftheriou E, Novack TA (2001) Current concepts: diffuse axonal injury-associated traumatic brain injury. Arch Phys Med Rehabil 82:1461–1471

Mikics E, Baranyi J, Haller J (2008) Rats exposed to traumatic stress bury unfamiliar objects—a novel measure of hyper-vigilance in ptsd models? Physiol Behav 94:341–348

Nakamura T, Hillary FG, Biswal BB (2009) Resting network plasticity following brain injury. PLoS One 4:e8220

O'Leary DD, Ruff NL, Dyck RH (1994) Development, critical period plasticity, and adult reorganizations of mammalian somatosensory systems. Curr Opin Neurobiol 4:535–544

Paxinos G, Watson C (1998) The rat brain in stereotaxic coordinates, vol 4. Academic Press, San Diego

Pitkanen A, Immonen RJ, Grohn OH, Kharatishvili I (2009) From traumatic brain injury to posttraumatic epilepsy: what animal models tell us about the process and treatment options. Epilepsia 50(Suppl 2):21–29

Povlishock JT (1986) Traumatically induced axonal damage without concomitant change in focally related neuronal somata and dendrites. Acta Neuropathol (Berl) 70:53–59

Prins ML (2008) Cerebral metabolic adaptation and ketone metabolism after brain injury. J Cereb Blood Flow Metab 28:1–16

Reeves TM, Phillips LL, Povlishock JT (2005) Myelinated and unmyelinated axons of the corpus callosum differ in vulnerability and functional recovery following traumatic brain injury. Exp Neurol 196:126–137

Rich KM, Yip HK, Osborne PA, Schmidt RE, Johnson EM Jr (1984) Role of nerve growth factor in the adult dorsal root ganglia neuron and its response to injury. J Comp Neurol 230:110–118

Rich KM, Disch SP, Eichler ME (1989) The influence of regeneration and nerve growth factor on the neuronal cell body reaction to injury. J Neurocytol 18:569–576

Royo NC, LeBold D, Magge SN, Chen I, Hauspurg A, Cohen AS, Watson DJ (2007) Neurotrophin-mediated neuroprotection of hippocampal neurons following traumatic brain injury is not associated with acute recovery of hippocampal function. Neuroscience 148:359–370

Sa MJ, Madeira MD, Ruela C, Volk B, Mota-Miranda A, Lecour H, Goncalves V, Paula-Barbosa MM (2000) Aids does not alter the total number of neurons in the hippocampal formation but induces cell atrophy: a stereological study. Acta Neuropathol (Berl) 99:643–653

Saatman KE, Contreras PC, Smith DH, Raghupathi R, McDermott KL, Fernandez SC, Sanderson KL, Voddi M, McIntosh TK (1997) Insulin-like growth factor-1 (igf-1) improves both neurological motor and cognitive outcome following experimental brain injury. Exp Neurol 147:418–427

Singleton RH, Povlishock JT (2004) Identification and characterization of heterogeneous neuronal injury and death in regions of diffuse brain injury: evidence for multiple independent injury phenotypes. J Neurosci 24:3543–3553

Singleton RH, Zhu J, Stone JR, Povlishock JT (2002) Traumatically induced axotomy adjacent to the soma does not result in acute neuronal death. J Neurosci 22:791–802

Smith DH, Chen XH, Xu BN, McIntosh TK, Gennarelli TA, Meaney DF (1997) Characterization of diffuse axonal pathology and selective hippocampal damage following inertial brain trauma in the pig. J Neuropathol Exp Neurol 56:822–834

Sofroniew MV, Cooper JD, Svendsen CN, Crossman P, Ip NY, Lindsay RM, Zafra F, Lindholm D (1993) Atrophy but not death of adult septal cholinergic neurons after ablation of target capacity to produce mrnas for ngf, bdnf, and nt3. J Neurosci 13:5263–5276

Sterio DC (1984) The unbiased estimation of number and sizes of arbitrary particles using the disector. J Microsc 134:127–136

Steward O (1989) Reorganization of neuronal connections following cns trauma: Principles and experimental paradigms. J Neurotrauma 6:99–152

Switzer RC III (2000) Application of silver degeneration stains for neurotoxicity testing. Toxicol Pathol 28:70–83

Tran LD, Lifshitz J, Witgen BM, Schwarzbach E, Cohen AS, Grady MS (2006) Response of the contralateral hippocampus to lateral fluid percussion brain injury. J Neurotrauma 23:1330–1342

Turrigiano GG (2008) The self-tuning neuron: Synaptic scaling of excitatory synapses. Cell 135:422–435

Turrigiano GG, Nelson SB (2004) Homeostatic plasticity in the developing nervous system. Nat Rev Neurosci 5:97–107

Uzan M, Albayram S, Dashti SG, Aydin S, Hanci M, Kuday C (2003) Thalamic proton magnetic resonance spectroscopy in vegetative state induced by traumatic brain injury. J Neurol Neurosurg Psychiatry 74:33–38

Waddell PA, Gronwall DM (1984) Sensitivity to light and sound following minor head injury. Acta Neurol Scand 69:270–276

Waite PME, Tracey DJ (1995) Trigeminal sensory system. In: Paxinos G (ed) The rat nervous system. Academic Press, San Diego

Warner MA, Youn TS, Davis T, Chandra A, de la Marquez PC, Moore C, Harper C, Madden CJ, Spence J, McColl R, Devous M, King RD, az-Arrastia R (2010) Regionally selective atrophy after traumatic axonal injury. Arch Neurol 67:1336–1344

West MJ (1993) New stereological methods for counting neurons. Neurobiol Aging 14:275–285

West MJ, Slomianka L, Gundersen HJG (1991) Unbiased stereological estimation of the total number of neurons in the subdivisions of the rat hippocampus using the optical fractionator. Anat Rec 231:482–497

West MJ, Ostergaard K, Andreassen OA, Finsen B (1996) Estimation of the number of somatostatin neurons in the striatum: An in situ hybridization study using the optical fractionator method. J Comp Neurol 370:11–22

Witgen BM, Lifshitz J, Smith ML, Schwarzbach E, Liang SL, Grady MS, Cohen AS (2005) Regional hippocampal alteration associated with cognitive deficit following experimental brain injury: a systems, network and cellular evaluation. Neuroscience 133:1–15

Woolsey TA, Van der LH (1970) The structural organization of layer iv in the somatosensory region (si) of mouse cerebral cortex. The description of a cortical field composed of discrete cytoarchitectonic units. Brain Res 17:205–242